(Received 19 January 2025, Accepted 5 March 2025, Scheduled 15 March 2025)

A Compact Ultra-Wideband Microstrip Antenna for Spectrum Monitoring

Yu Liu[1], Shuo Yu[1,2], and Xiaoming Liu[1,2,*]

[1] *The School of Physics and Electronic Information, Anhui Normal University, Wuhu 241002, China*
[2] *Anhui Provincial Engineering Center on Information Fusion and Control of Intelligent Robot, Wuhu 241002, China*

ABSTRACT: A compact ultra-wideband antenna fed by coplanar waveguide is reported in this paper. The designed antenna consists of a trumpet-shaped planar radiation patch and a symmetrical ground patch. Two Mickey-Mouse shaped perturbative slots and two quarter-elliptical grooves are etched on the ground to obtain better impedance matching. By prolonging the radiation patch, a very wide −10 dB bandwidth of covering 300 MHz–18 GHz with bandwidth ratio up to 60 : 1 and omnidirectional coverage are achieved. Furthermore, the proposed antenna is able to cover P(0.3-1G), L(1-2G), S(2-4G), C(4-8G), X(8-12G), and Ku (12-18G) bands, which is much preferred for wideband spectrum monitoring.

1. INTRODUCTION

Spectrum monitoring techniques have been intensively investigated either to ensure legal use of radio spectrum or evaluate the working electromagnetic environment prior to or after deployment of electronic instruments [1]. To monitor potential harmful electromagnetic signals, the receiving antenna is one of the key components. Particularly, its bandwidth is preferred as wide as possible. Therefore, the development of ultra-wideband (UWB) antenna is a priority in system design for spectrum monitoring.

Conventional UWB antennas are typically designed to cover the frequency range of 3.1 GHz–10.6 GHz [3–8], which is pretty much dedicated by the IEEE Std 802.15.4a-2007. However, the antenna in spectrum monitoring has much more stringent requirement on bandwidth [2]. For instance, in this work, the required prototype has a very low operating frequency down to 300 MHz, and relatively high frequency up to 18 GHz to be realized in a single antenna. It is seen that the frequency ratio is up to 60 : 1. To develop such types of UWB antenna, there are many designs that have been reported [9–14]. However, the difficulties of these UWB antennas are operating above 3 GHz, which apparently does not meet the requirement of this work. To further push down the working frequency, a growing number of UWB antennas capable of working in the sub-3 GHz have emerged [15–24]. Although the frequency has been commonly expanded to 1 GHz in recent developments, which is not close enough to 300 MHz target.

On the other hand, these antennas are not sufficiently compact. For instance, an ultra-wideband low-profile antenna is proposed in [15]. Though it has a bandwidth of 0.1 GHz–3 GHz, the antenna size measures $310 \times 310 \times 0.8\,\text{mm}^3$, which is considerably large and unsuitable for spectrum monitoring operation. In addition, it fails to cover the spectrum beyond 3 GHz. It is seen that such frequency coverage is insufficient for current spectrum monitoring antennas. In summary, the miniaturization of UWB antenna with very high frequency ratio requires further efforts.

Technically, the aforementioned works do provide many promising methods for compact UWB antenna design. For example, the coplanar waveguide (CPW)-fed UWB antenna stands out for its simplicity, ease of integration, and ability to achieve wide bandwidth with enhanced impedance matching. This technique has become a popular approach to optimization of the performance of a UWB antenna [20–24]. A CPW-fed dual band notched UWB antenna is proposed in [21]. However, spectrum monitoring antennas are required to obtain as wide working frequency as possible to ensure comprehensive monitoring of the available spectrum. It is generally undesirable to incorporate band-notch designs. In addition, the miniaturization methods in [23] and [24] are very instructive. By taking these techniques to one design, it is very likely to reach a qualified antenna meeting all the specifications of this work.

In this work, a compact CPW-fed antenna with wide bandwidth is designed, fabricated, and measured. By extending the length of radiation patch and engraving slots on the ground patch properly, the antenna achieves a −10 dB bandwidth of at least 196% (300 MHz–18 GHz) with ratio bandwidth more than 60 : 1. The good radiation performances of the antenna can be verified by experimental tests. Details of the antenna design and measurement results are presented and analyzed in the following section.

2. ANTENNA DESIGN AND ANALYSIS

The configuration of the proposed UWB antenna is depicted in Fig. 1, and a single-layer structure antenna is investigated. Both the radiator and ground are depicted using orange part located on the top of the gray part which is a 1.6 mm thick FR4

* Corresponding author: Xiaoming Liu (xiaoming.liu@ahnu.edu.cn).

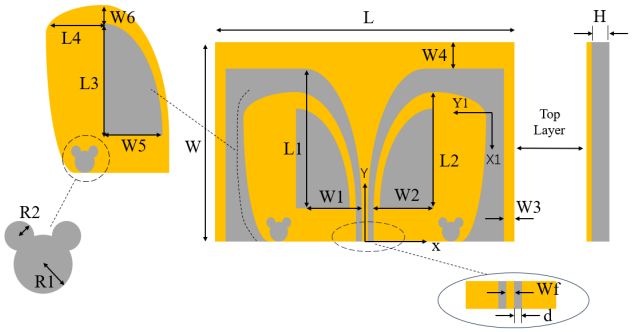

FIGURE 1. Specific geometric features of the antenna design.

Parameter	Value	Parameter	Value
L	168	W_1	42
W	120	W_2	42
H	1.6	W_3	2
L_1	96	W_4	12
L_2	84	W_5	36
L_3	66	R_1	4
L_4	30	R_2	2

TABLE 1. Dimension of the proposed antenna (unit: mm).

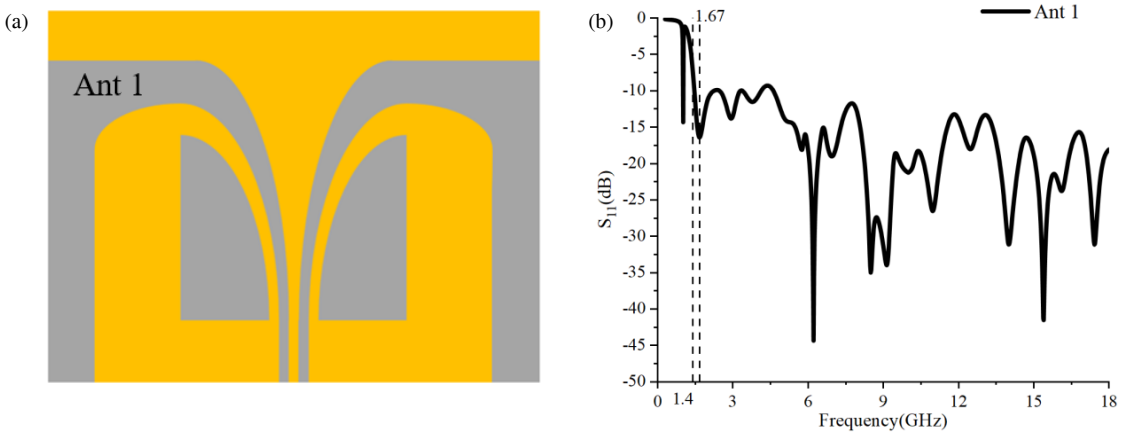

FIGURE 2. The configuration and simulation of Ant 1.

substrate (relative permittivity of 4.4 and loss tangent of 0.02) with a dimension of $168 \times 120\,\text{mm}^2$. The antenna is fed using a coplanar waveguide feeding structure.

Detailed dimensions of the proposed antennas are shown in Table 1 and Fig. 1. The antenna consists of a prolonged trumpet-shaped planar radiation patch and a symmetrical ground patch. Smooth layout of the designed antenna is essential, aiming to broaden the operating bandwidth. The edge of the radiator patch linked with the feeding structure and the upper corner of the ground plane are formed by two pairs of symmetrical quarter ellipses with different sizes. To allow the UWB antenna to work in considerably low frequency, the length of both sides of the radiating patch are extended by two rectangular slices with widths W_3 and W_4. Two Mickey-Mouse shaped perturbed slots and two quarter elliptical grooves are etched on the ground symmetrically to obtain better impedance matching in such a wide frequency band. The optimized parameters of each part of the antenna are listed in Table 1.

Four steps are followed to yield the required broad bandwidth. The proposed antenna originated from Ant 1 is depicted in Fig. 2(a). The radiation patch length in Ant 1 was not extended, and it consists of two quarter-elliptical slots. Fig. 2(b) shows the operating bandwidth of the antenna in Ant 1. By contrast, it is apparent that the low cutoff frequency of Ant 1 is around 1.4 GHz, which does not meet the required cutoff frequency in this paper. For lower cutoff frequency and better impedance matching, it is necessary to modify the initial configuration design.

As stated previously, round corner is helpful for pushing down the working frequency. Fig. 3(a) reveals the revised design with round corners (Ant 2). The simulation result of Ant 2 is shown in Fig. 3(b). It is seen that both Ant 1 and Ant 2 generate a resonance frequency around 1.67 GHz. But Ant 2 with round corner causes a significant reduction on S_{11} curve and pushes the low cutoff frequency from 1.4 GHz down to 1 GHz.

Figure 4 shows the configuration and simulation results of Ant 3. By adding two stub lines to the radiation patch at each side, the low frequency takes place at 580 MHz. This is very encouraging since it is very close to 300 MHz.

At last, two Mickey-Mouse shaped perturbing slots are introduced into the bottom of Ant 3 ground as pictured in Fig. 5(a). The introduction of perturbing slots effectively alters the current distribution in the ground plane and thus results in enhanced impedance in the low frequency range. Eventually, through optimization of the whole structure, a working bandwidth from 300 MHz to 18 GHz is achieved for the proposed UWB antenna, as presented in Fig. 5(b).

3. PARAMETRIC STUDY

A parametric study has been conducted to examine the effect of each parameter. We only present the range from 300 MHz to 7 GHz, since the influence of the structural parameters is

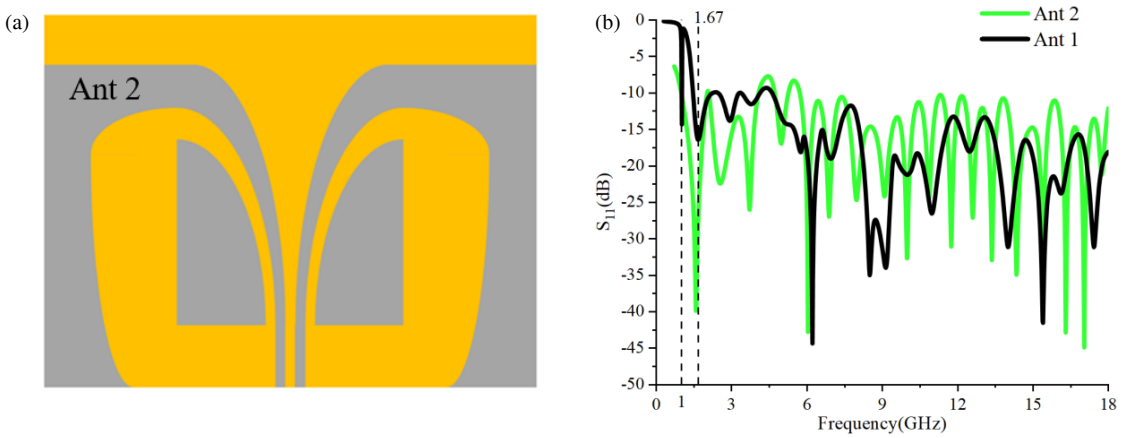

FIGURE 3. The configuration and simulation results of Ant 2.

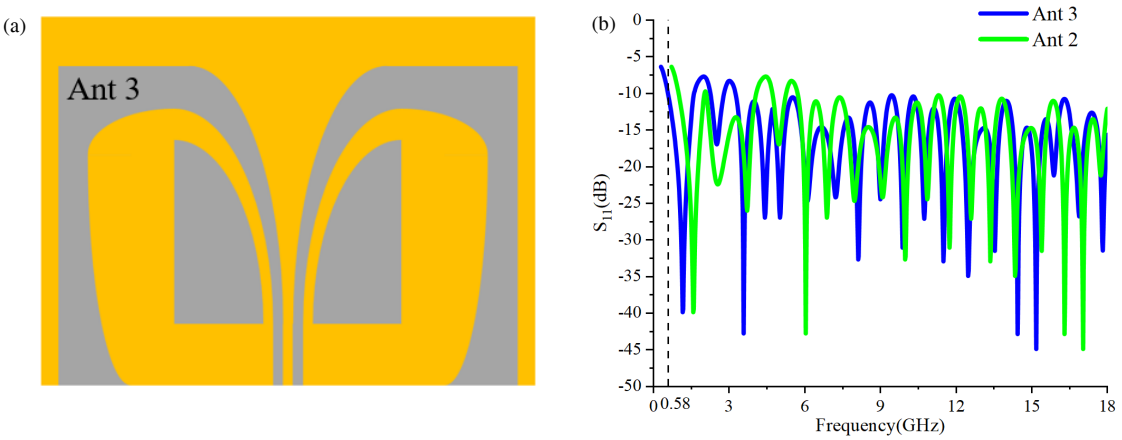

FIGURE 4. The configuration and simulation of Ant 3.

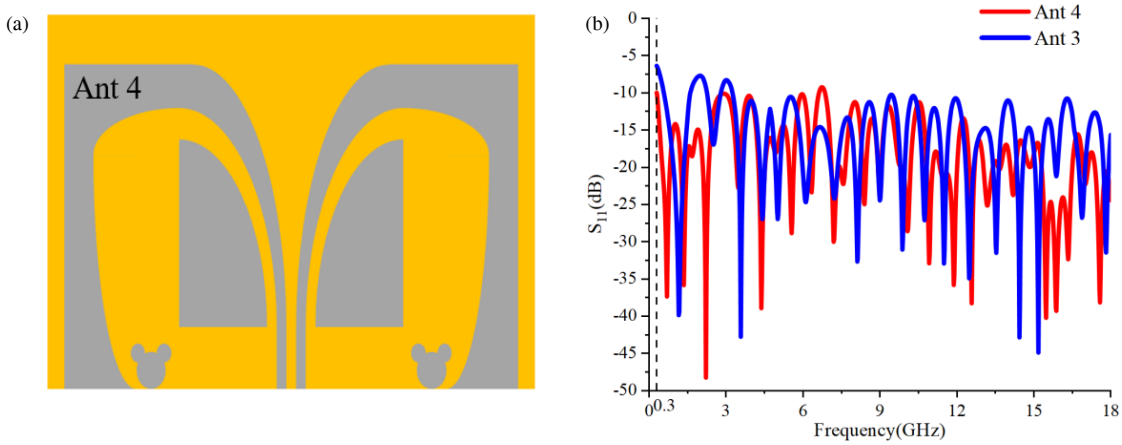

FIGURE 5. The configuration and simulation of the proposed antenna (Ant 4).

not pronounced beyond 7 GHz. Fig. 6 demonstrates the effect of W_3 on S_{11}. With the increase of W_3, the low cutoff frequency shifts to the lower frequency band. However, when $W_3 > 2$ mm, the effect is deteriorated. Based on this observation, the value of the width of W_3 is adjusted to 2 mm.

As shown in Fig. 7, parameter m for the exponential curve $y_1 = 5 \times e^{m \times x_1}$ significantly influences the lowest operating frequency of the antenna. As m increases, the cutoff frequency decreases, leading to a shift towards lower frequency. However, further increases in m cause the lowest frequency to rise again.

The influence due to L_3 and W_5 is analyzed in Fig. 8. The results indicate that both the changes of L_3 and W_5 exert little influence on improving impedance matching or lowering the cutoff frequency.

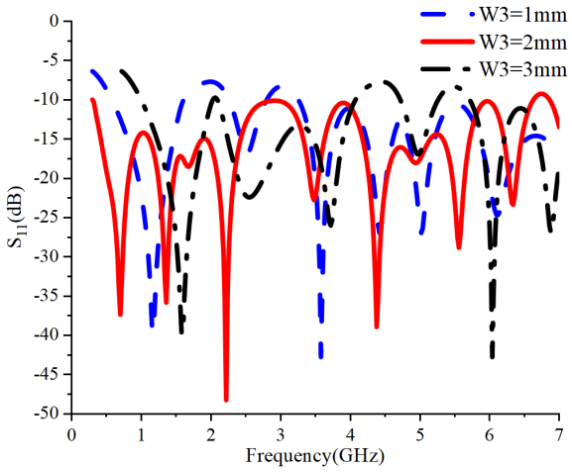

FIGURE 6. Effect of W_3 on antenna performance.

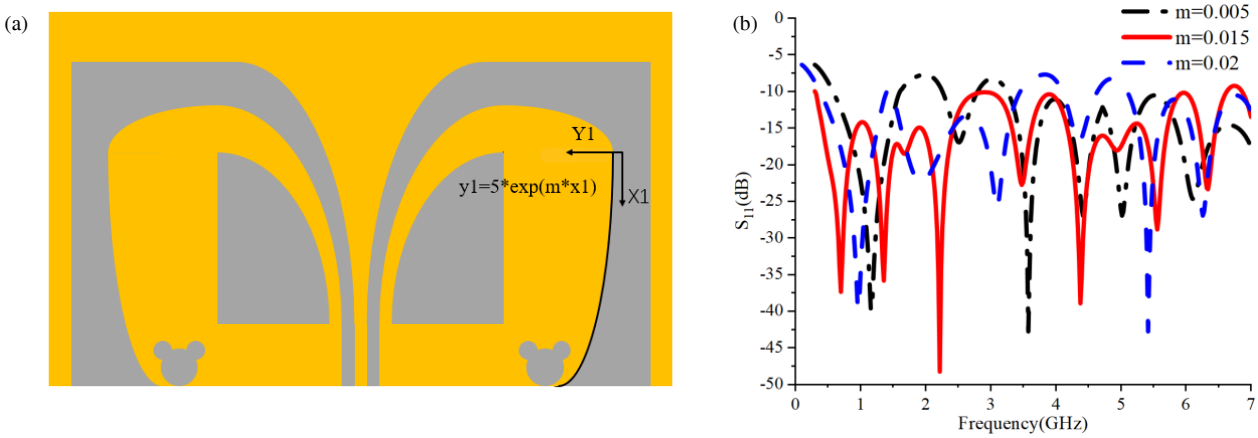

FIGURE 7. Effect of parameter m on antenna performance.

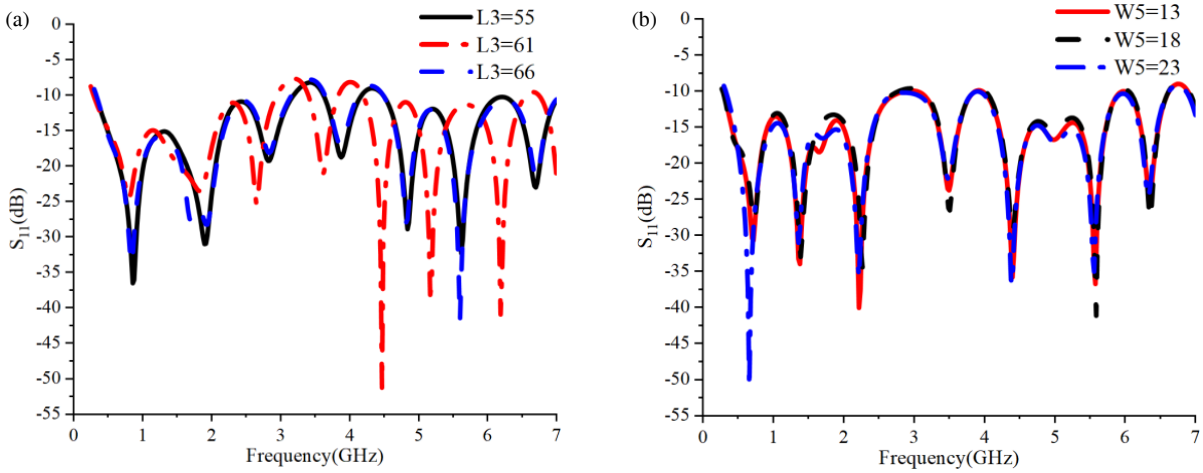

FIGURE 8. Effect of L_3 and W_5 on antenna performance: (a) L_3; (b) W_5.

4. MEASUREMENT AND DISCUSSION

The fabricated antenna is shown in Fig. 9. Simulations of the proposed antenna were conducted by HFSS. To verify the working performance of the fabricated antenna, a vector network analyzer was used to measure the S_{11}, while the radiation pattern was measured in a microwave anechoic chamber, as shown in Fig. 10. Fig. 11 plots the comparison between simulated and measured reflection coefficients. The simulated and measured results indicate that the antenna has a well-matched -10 dB impedance bandwidth from 300 MHz to higher than

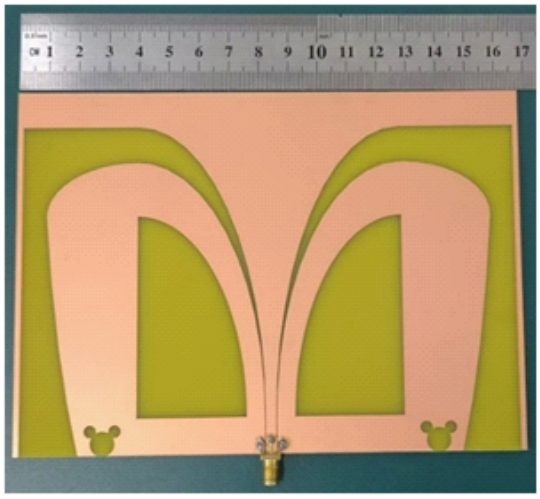

FIGURE 9. Photograph of the fabricated antenna.

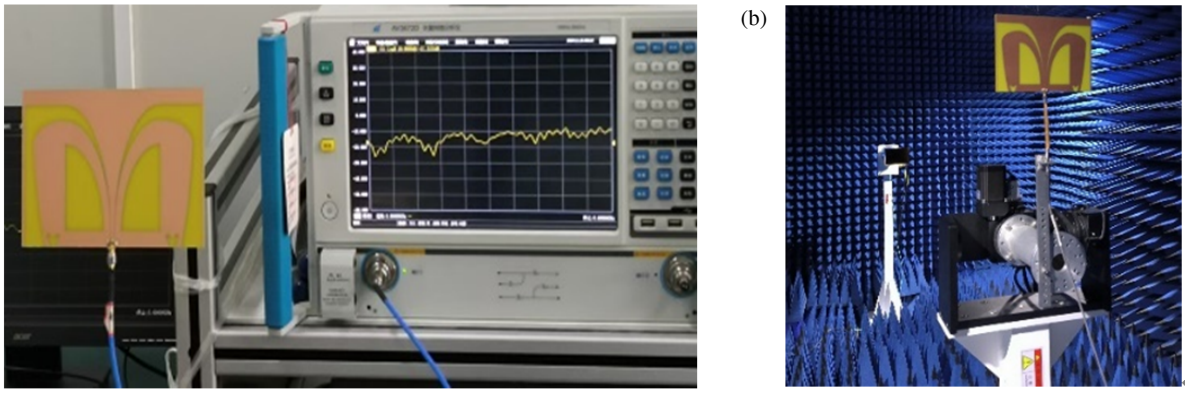

FIGURE 10. Antenna measurement. (a) S_{11}; (b) far field test.

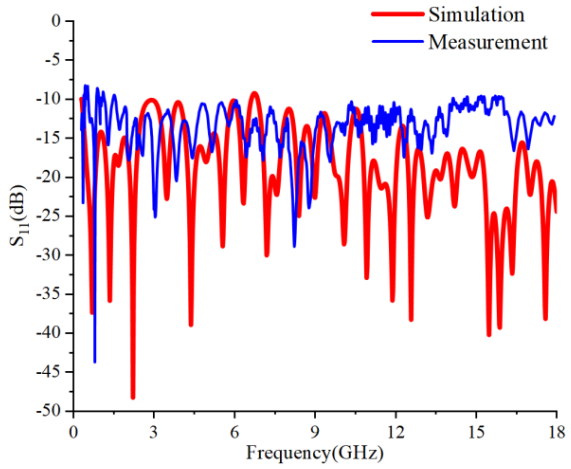

FIGURE 11. Comparison of simulation and measurement results.

18 GHz, and the bandwidth ratio is greater than 60 : 1. Due to the limitation of the measurement equipment, the radiation pattern was measured only within the frequency range from 2 GHz to 12 GHz. The simulated and measured radiation patterns are plotted in Fig. 12. It has to be mentioned that the "E-plane" means "xz-plane", and "H-plane" means "xy-plane". Gain and radiation efficiency are plotted in Fig. 13. It can be observed that the peak gain is 4.9 dB through the working bandwidth, while the radiation efficiency rises from 22% to 97%.

Comparison of the proposed antenna with other published designs is listed in Table 2. Here, the wavelength λ_0 refers to the low cutoff frequency of -10 dB bandwidth. By contrast, the designed antenna has lower operating frequency than any other design. In addition, a bandwidth of 17.7 GHz is obtained, corresponding to a bandwidth ratio of 60 : 1. Furthermore, the electrical size of this antenna is $0.17\lambda_0 \times 0.12\lambda_0$, which is smaller than that in [23] while this design provides a much larger bandwidth ratio, covering the P(0.3-1G), L(1-2G), S(2-4G), C(4-8G), X(8-12G), and Ku (12-18G) bands.

Adding two stubs alters the current distribution, leading to a longer effective current path, which lowers the resonant frequency and broadens the impedance bandwidth. The introduction of Mickey-Mouse shaped perturbing slots serves dual purposes: enhancing impedance matching and improving radiation efficiency. Perturbing slots create localized electromagnetic field perturbations that introduce controlled inductive or capacitive effects. These effects counteract unwanted reactance, resulting in a closer alignment of input impedance

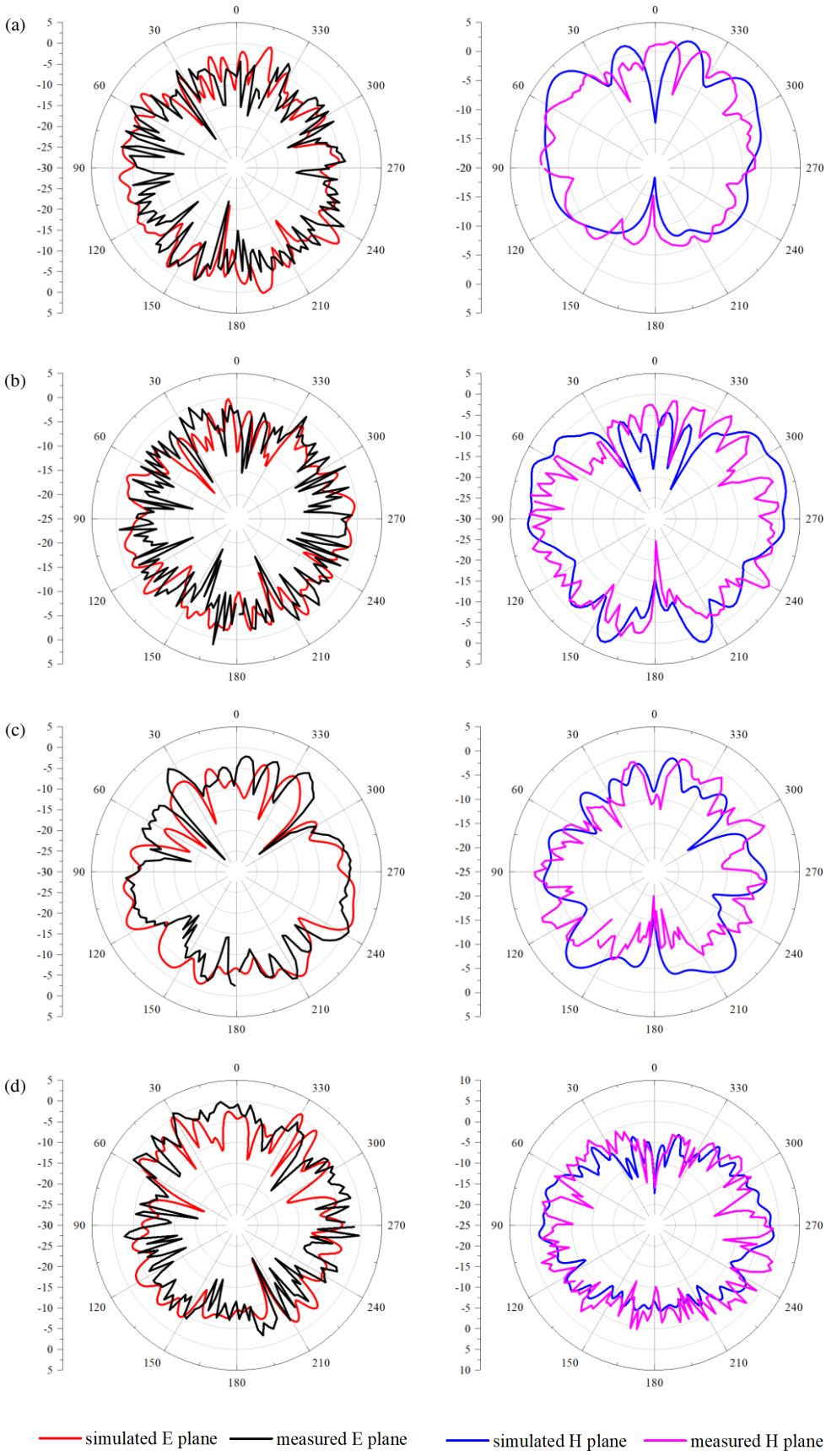

FIGURE 12. The simulated and measured radiation patterns in E-plane and H-plane at (a)2 GHz; (b) 5 GHz; (c) 9 GHz; (d) 12 GHz.

TABLE 2. Comparison of the proposed UWB Antenna and other designs.

Ref.	Size (mm^3)	Size ($\lambda_0 \times \lambda_0$)	$S_{11} < -10$ dB GHz	Relative Bandwidth	Bandwidth ratio
[4]	$60 \times 60 \times 0.8$	0.7×0.7	3.5–9.5	92%	2.7 : 1
[15]	$310 \times 270 \times 0.8$	0.1×0.09	0.1–3	187%	30 : 1
[18]	$77 \times 35 \times 1.6$	0.37×0.17	1.44–18.8	172%	13 : 1
[19]	$140 \times 66 \times 1.5$	0.93×0.44	2–32	176%	16 : 1
[20]	$100 \times 80 \times 1.5$	0.33×0.27	1–15	175%	15 : 1
[23]	$140 \times 100 \times 1$	0.19×0.13	0.4–20	192%	50 : 1
[24]	$22 \times 13 \times 0.8$	0.21×0.12	2.82–13.25	130%	4.7 : 1
This work	$168 \times 120 \times 1.6$	0.17×0.12	0.3–18	193%	60 : 1

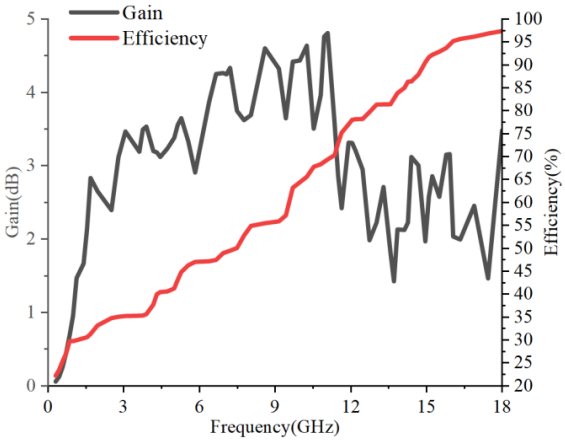

FIGURE 13. Gain and radiation efficiency of Ant 4.

with the desired impedance, typically 50 ohms. Moreover, the slots contribute to broadband operation by enabling better coupling between different resonant modes, which aids in achieving a wider bandwidth. Additionally, the perturbations influence current redistribution, which can improve radiation pattern stability and minimize sidelobe levels.

5. CONCLUSIONS

A novel UWB antenna for spectrum sensing was proposed. By prolonging the length of the radiation patch symmetrically and properly adjusting the width of the extended radiating patch, the operating frequency ranging from 300 MHz to 18 GHz can be achieved. By introducing Mickey-Mouse shaped perturbed slots, the impedance matching is effectively improved on such broad frequency band. This design shows omnidirectional coverage and can cover P, L, S, C, X, Ku bands for wideband spectrum sensing application.

ACKNOWLEDGEMENT

This work is supported in part by the Natural Science Foundation of Anhui Province (2308085Y02) and the National Natural Science Foundation of China (61871003).

REFERENCES

[1] McCarthy, D., "Modern Receiver Architectures: Considerations for spectrum monitoring applications," in *2019 IEEE International Symposium on Electromagnetic Compatibility, Signal & Power Integrity (EMC+SIPI)*, 18–21, New Orleans, LA, USA, Jul. 2019.

[2] Bhopale, N. I. and S. N. Pawar, "Challenges for designing a multiband Ultra-Wide Band (UWB) antenna with its solutions," in *2022 International Conference on Disruptive Technologies for Multi-Disciplinary Research and Applications (CENTCON)*, Vol. 2, 87–91, Bengaluru, India, Dec. 2022.

[3] Nella, A. and A. S. Gandhi, "A five-port integrated UWB and narrowband antennas system design for CR applications," *IEEE Transactions on Antennas and Propagation*, Vol. 66, No. 4, 1669–1676, Feb. 2018.

[4] Bahrami, S., G. Moloudian, H.-J. Song, and J. L. Buckley, "Reconfigurable UWB circularly polarized slot antenna with three modes of operation and continuous tuning rang," *IEEE Transactions on Antennas and Propagation*, Vol. 70, No. 9, 8542–8547, Sep. 2022.

[5] Chen, Y., Y. He, W. Li, L. Zhang, S.-W. Wong, and A. Boag, "A 3-9 GHz UWB high-gain conformal end-fire Vivaldi antenna array," in *2021 IEEE International Symposium on Antennas and Propagation and USNC-URSI Radio Science Meeting (APS/URSI)*, 737–738, Singapore, Dec. 2021.

[6] Doddipalli, S. and A. Kothari, "Compact UWB antenna with integrated triple notch bands for WBAN applications," *IEEE Access*, Vol. 7, 183–190, Dec. 2018.

[7] Park, S. and K.-Y. Jung, "Novel compact UWB planar monopole antenna using a ribbon-shaped slot," *IEEE Access*, Vol. 10, 61 951–61 959, Jun. 2022.

[8] Khan, A. S., K. Gorai, and S. Kundu, "A compact planar microstrip patch antenna in commercial ultra-wideband spectrum," in *2023 IEEE Microwaves, Antennas, and Propagation Conference (MAPCON)*, 1–4, Ahmedabad, India, Dec. 2023.

[9] Gupta, A. and M. L. Meena, "Design of semi circular floral shape directive UWB antenna for radar based microwave imaging," in *2021 International Conference on Artificial Intelligence and Smart Systems (ICAIS)*, 1188–1192, Coimbatore, India, Mar. 2021.

[10] Rafique, U., S. Agarwal, S. M. Abbas, P. Dalal, R. Ullah, and S. H. Kiani, "Circular ring fractal UWB antenna for microwave imaging applications," in *2023 IEEE Wireless Antenna*

and Microwave Symposium (WAMS), 1–4, Ahmedabad, India, Jun. 2023.

[11] Ouf, E. G., K. F. A. Hussein, A. E. Farahat, and S. A. Mohassieb, "Super-wide band antenna on three-layer substrate for microwave and millimeter-wave applications," in *2023 International Telecommunications Conference (ITC-Egypt)*, 58–65, Alexandria, Egypt, Jul. 2023.

[12] Chu, S., M. N. Hasan, J. Yan, and C. C. Chu, "A planar super wideband annular ring monopole antenna with time domain characterization," in *2018 Asia-Pacific Microwave Conference (APMC)*, 1573–1575, Kyoto, Japan, Nov. 2018.

[13] Suganya, E., T. A. J. M. Pushpa, and T. Prabhu, "Design and analysis of circular patch antenna for microwave applications," in *2023 International Conference on Applied Intelligence and Sustainable Computing (ICAISC)*, 1–4, Dharwad, India, Jun. 2023.

[14] Khan, A. S., K. Gorai, and S. Kundu, "A compact planar microstrip patch antenna in commercial ultra-wideband spectrum," in *2023 IEEE Microwaves, Antennas, and Propagation Conference (MAPCON)*, 1–4, Ahmedabad, India, Dec. 2023.

[15] Qi, Y., B. Yuan, Y. Cao, and G. Wang, "An ultrawideband low-profile high-efficiency indoor antenna," *IEEE Antennas and Wireless Propagation Letters*, Vol. 19, No. 2, 346–349, Feb. 2020.

[16] Al-Hammami, K. A., A.-R. S. Omar, M. M. Qwakneh, and Y. S. Faouri, "Frequency reconfigurable super wide band hexagonal patch antenna," in *2020 Global Congress on Electrical Engineering (GC-ElecEng)*, 129–133, Valencia, Spain, Sep. 2020.

[17] Gite, S. S. and M. B. Kadu, "A compact slotted ellipse ultra-wideband antenna (UWB) for detection applications," in *2021 International Conference on Smart Generation Computing, Communication and Networking (SMART GENCON)*, 1–4, Pune, India, Oct. 2021.

[18] Chen, K.-R., C.-Y.-D. Sim, and J.-S. Row, "A compact monopole antenna for super wideband applications," *IEEE Antennas and Wireless Propagation Letters*, Vol. 10, 488–491, May 2011.

[19] Nassar, I. T. and T. M. Weller, "A novel method for improving antipodal vivaldi antenna performance," *IEEE Transactions on Antennas and Propagation*, Vol. 63, No. 7, 3321–3324, May 2015.

[20] Agrawal, S., "A CPW-fed super wideband dielectric resonator antenna," in *2020 IEEE International Conference on Advanced Networks and Telecommunications Systems (ANTS)*, 1–5, New Delhi, India, Dec. 2020.

[21] Hadda, L., S. K. Yadav, N. Gupta, S. Kumar, and A. K. Singh, "Compact reconfigurable dual band notched UWB antenna," in *2023 11th International Conference on Intelligent Systems and Embedded Design (ISED)*, 1–4, Dehradun, India, Dec. 2023.

[22] Agrawal, S., "A CPW-fed band notch super wideband antenna with Scale up/down capability," in *2023 IEEE Microwaves, Antennas, and Propagation Conference (MAPCON)*, 1–6, Ahmedabad, India, Dec. 2023.

[23] Yang, L., D. Zhang, X. Zhu, and Y. Li, "Design of a super wide band antenna and measure of ambient RF density in urban area," *IEEE Access*, Vol. 8, 767–774, 2019.

[24] Nan, J., J. Zhao, M. Gao, W. Yang, M. Wang, and H. Xie, "A compact 8-states frequency reconfigurable UWB antenna," *IEEE Access*, Vol. 9, 144 257–144 263, 2021.